Improving Source-Free Target Adaptation with Vision Transformers Leveraging Domain Representation Images

Gauransh Sawhney[1*], Daksh Dave[2], Adeel Ahmed[3], Jiechao Gao[4*], Khalid Saleem[5]

[1,2]Department of Electrical Electronics, BITS Pilani-Pilani campus, Rajasthan, India .
[3,5]Department of Computer Science, Quaid-i-Azam University, Islamabad 45320, Pakistan .
[4]Department of Computer Science, University of Virginia, Charlottesville, VA, United States .

*Corresponding author(s). E-mail(s): f20180325@pilani.bits-pilani.ac.in; jg5ycn@virginia.edu;

Abstract

Unsupervised Domain Adaptation (UDA) methods facilitate knowledge transfer from a labeled source domain to an unlabeled target domain, navigating the obstacle of domain shift. While Convolutional Neural Networks (CNNs) are a staple in UDA, the rise of Vision Transformers (ViTs) provides new avenues for domain generalization. This paper presents an innovative method to bolster ViT performance in source-free target adaptation, beginning with an evaluation of how key, query, and value elements affect ViT outcomes. Experiments indicate that altering the key component has negligible effects on Transformer performance. Leveraging this discovery, we introduce Domain Representation Images (DRIs), feeding embeddings through the key element. DRIs act as domain-specific markers, effortlessly merging with the training regimen. To assess our method, we perform target adaptation tests on the Cross Instance DRI source-only (SO) control. We measure the efficacy of target adaptation with and without DRIs, against existing benchmarks like SHOT-B* and adaptations via CDTrans. Findings demonstrate that excluding DRIs offers limited gains over SHOT-B*, while their inclusion in the key segment boosts average precision promoting superior

domain generalization. This research underscores the vital role of DRIs in enhancing ViT efficiency in UDA scenarios, setting a precedent for further domain adaptation explorations.

Keywords: Unsupervised Domain Adaptation, Vision Transformers, Domain Representation Image, Computer Vision, Key Redundancy, Neural Networks

1 Introduction

Deep Neural Networks have exhibited remarkable performance across various applications, yet they often struggle to generalize well to new domains due to the domain shift problem [1],[2],[3], and [4]. Unsupervised Domain Adaptation (UDA) techniques have emerged as a powerful approach to address this challenge, aiming to transfer knowledge from a labeled source domain to an unlabeled target domain that differs from the source.

Conventionally, UDA methods have relied on learning domain-invariant features using Convolutional Neural Networks (CNNs). However, with the recent success of Vision Transformers (ViTs) [5] in various computer vision tasks [6], there is a growing interest in leveraging ViTs for UDA. The unique characteristics of ViTs, such as their ability to capture long-range dependencies and their adaptability across domains, make them a promising alternative to CNN-based frameworks.

In this research, we aim to explore the potential of Vision Transformers in the context of UDA. Specifically, we investigate the impact of introducing perturbations in the key component of ViTs, considering its relatively minor effect on the overall performance of Transformers. Building upon this observation, we propose a novel approach called Domain Representation Images (DRIs) that involves passing embeddings through the key to enhancing the domain generalization capability of source-only (SO) models. Our contributions can be summarized as follows:

- We analyze key redundancy in transformers and its impact on domain adaptation. By examining the range of key values across layers, we gain insights into their distribution. Our experiments show that substituting the key with a domain-specific embedding does not hinder model performance, and provides improved representation of domain-specific images.
- We introduce the concept of DRIs as a means to improve the domain generalization of source-only baselines and enhance target adaptation performance in a source-free setting.

To assess the efficacy of our proposed method, we undertook comprehensive experiments on a public UDA datasets, Office-Home[7], Office-31 [8] and VisDA [9]. The outcomes indicate that our method surpasses existing source-free baselines, such as SHOT-B*[10], attaining state-of-the-art results in target adaptation.

2 Literature Review

Deep Neural Networks (DNNs) have garnered substantial success in a plethora of applications. Nonetheless, their generalization capabilities across novel domains remain an obstacle, primarily due to the issue of domain shift [1],[2],[3], and [4]. In response, significant research endeavors have been channeled into Domain Adaptation [11], [12], [13], and [14].

Domain Adaptation approaches are typically classified according to the labeling status of the target dataset. In a supervised context, labels fully annotate the target dataset, whereas the semi-supervised context comprises both labeled and unlabeled data [15]. Conversely, the unsupervised approach operates under the premise that the target dataset lacks labels entirely [16]. Furthermore, Domain Adaptation strategies diverge into closed-set [8] and open-set [17] categories. The former pertains to instances where source and target datasets share identical classes, while the latter involves datasets with disparate and non-overlapping classes. Additionally, Domain Adaptation methodologies are delineated based on source data availability during target adaptation. Source-free adaptation pertains to conditions where only the source pre-trained model is available during target adaptation. In contrast, non-source-free (NSF) adaptation entails accessibility to both the source data and the pre-trained model in the course of target adaptation.

While earlier works on source-free adaptation were limited to self-supervised domain adaptation, recent attention has been devoted to source-free UDA for deep neural networks [18]. For instance, one approach proposes a framework that freezes the classifier layer and fine-tunes the model using information maximization and pseudo-labeling, even extending to multi-source settings [18]. Another framework focuses on black-box source models by splitting the target data and employing semi-supervised learning [19]. They further propose the SHOT framework for source-free settings, leveraging information maximization for learning target-specific feature encoding. Additionally, they introduce the SHOT++ framework, which incorporates a novel label-transferring strategy based on the confidence of label predictions.

Existing UDA approaches primarily focus on aligning the source and target distributions and learning domain-invariant features. Methods such as domain adversarial learning [20],[21], and [22] and discrepancy minimization [23], and [24] aim to achieve domain alignment. These methods however are non-source-free in nature. Additionally, another line of UDA methods [25], [26], [27], and [28] involves developing regularization terms for implicit domain alignment, domain-specific normalization-based approaches, and feature regularization-based methods.

Several studies [29], [30],[31], [32], and [33] have investigated the integration of federated learning into domain adaptation scenarios. In multi-source-free domain adaptation, the constraint that prevents data and parameter transmission across different source domains is not required. However, it is worth noting that current federated learning studies typically generate a common model for all clients without considering the heterogeneity of data distribution among different clients. This limitation suggests the need for further research to address the challenges posed by varying client data.

The concept of test-time adaptation [34],[35],[36], and [37] has also been explored, focusing on adapting the source model to the target domain during the inference

procedure. However, existing approaches often rely on accessing batch-sized (¿1) target samples during inference, making it difficult to handle scenarios where target samples arrive one by one sequentially. This limitation calls for the development of methods capable of adapting to sequential and incremental target samples, which can be more practical and efficient in real-world applications.

Black-box Source-Free Unsupervised Domain Adaptation (SFUDA) methods face challenges due to the unavailability of the structure and parameters of the target model. Consequently, these methods often require the manual design of a target model. For instance, Liu et al. [38] employed a U-Net-based framework for segmentation as the target model. However, such manually designed architectures may not always be suitable for effective adaptation to the target domain. This highlights the need for automated or more adaptive approaches to target model design in black-box SFUDA methods.

In recent years, source-free domain adaptation within semi-supervised frameworks, involving a minimal quantity of labeled target data during model training, has garnered increased interest [39], [40]. This method characteristically merges semi-supervised adaptation strategies with active learning [41], [42], revelations of model memorization [43], and the principles of consistency and diversity learning [44]. Despite advancements in this field, opportunities for enhancement persist, especially concerning the optimization of scarce labeled target samples.

While most existing works in UDA utilize CNN-based architectures, the emergence of Vision Transformers (ViTs) [45] has garnered attention in computer vision tasks. Vision Transformers, with their ability to capture long-range dependencies among visual features, have shown promising results in detection, segmentation, and classification tasks. ViTs have also started to receive attention in UDA. For example, one study proposes a framework based on ViT's adaptability across domains, incorporating a Transferable and Adaptive Module (TAM) to capture transferable and discriminative features [10]. Another work introduces a 3-branch framework, CDTrans, with cross-attention in the middle branch and a two-way center labeling method for producing high-quality pseudo-labels [10]. Patch-Mix [46] intends to further improve upon CDTrans by building an intermediate domain by sampling from source and target domains using game-theoretical models.

However, the aforementioned works predominantly focus on non-source-free adaptation, and the exploration of source-free domain adaptation in transformers remains relatively unexplored. Our work aims to fill this research gap by leveraging the CDTrans framework for source pretraining and integrating transformers into the SHOT codebase. Our methodology involves utilizing a DeiT-base [47] model consisting of 12 attention layers, pre-trained on the ImageNet 1k dataset [48], [49]. Additionally, we draw insights from recent studies on domain-adaptive training techniques [21] to enhance the performance of transformers in source-free target adaptation. By incorporating these advancements, we aim to improve the generalization capabilities of transformers in handling domain shifts and achieving better adaptation results.

In summary, the literature on UDA encompasses a wide range of approaches, including domain alignment techniques and regularization-based methods. While earlier works primarily focused on CNN-based architectures, recent advancements in

Vision Transformers have shown promise in various computer vision tasks. However, the exploration of source-free adaptation in transformers is relatively limited. Our work contributes to the field by investigating source-free UDA using ViTs and introduces the concept of Domain Representation Images to enhance domain generalization capabilities. The findings pave the way for further research in key redundancy and other methods for generating DRIs to improve target adaptation performance.

3 Proposed Methodology

The proposed methodology for the Domain Representation Image (DRI) in the DeiT model is visually depicted in Fig. 1. The process begins with the input image being paired with a DRI Image, which incorporates image augmentation techniques. These paired images are then passed through the first transformer encoder, where they undergo transformation into patch embeddings and are further processed to generate Key (K), Query (Q), and Value (V) representations. In the subsequent step, the Key derived from the DRI image and the Query and Value obtained from the input image are utilized for multi-head self-attention. Prior to feeding them into a multi-layered perceptron (MLP), the outputs of the self-attention mechanism are normalized. The resulting output is then fed into the next transformer encoder to continue the encoding process.

3.1 Image Augmentation

In the first step in our proposed methodology framework, we use Image Augmentation as part of the Domain Representation Image (as shown in Fig. 1). Image augmentation [50] is a widely used technique in training machine learning models, particularly in computer vision tasks. It involves artificially generating new images by applying various transformations to the existing images. Common augmentations include rotation, horizontal flip, scaling, cropping, and color adjustments.

In the context of our study, we explore the effects of image augmentation on the domain generalizability of transformers. We employ five custom augmentations, as shown in Fig. 2, to construct the Domain Representation Image:

- Cartoon [51]: This technique aims to transform the appearance of images to resemble a cartoon-like style, by altering the style to be more cartoonish, the augmented images exhibit exaggerated features, bold outlines, and vibrant colors typically associated with cartoons.
- Weather [51]: This technique aims to simulate various weather conditions by adding elements such as clouds, fog, snowflakes, or rainfall to the original image.
- AdaIN [52]: AdaIN (Adaptive Instance Normalization) is an image augmentation technique that dynamically adjusts the style and content of an image by matching the statistics of the content image to that of the style image, allowing for style transfer and domain adaptation.
- Fourier Domain Adaptation (FDA) [53]: FDA is an image augmentation technique that operates in the Fourier domain, transforming images into frequency representations and applying domain adaptation techniques to align the distribution of

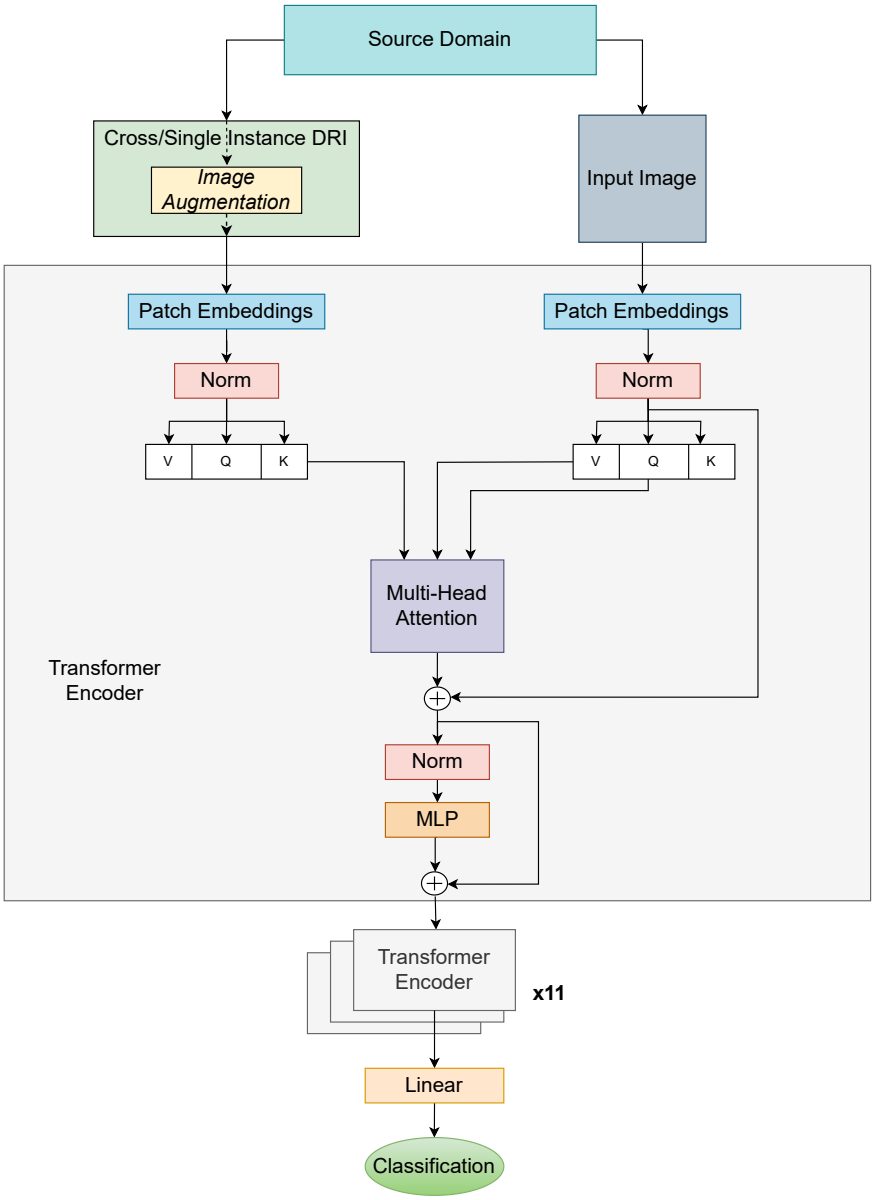

Fig. 1 Illustration of DRI in transformers.

frequencies between source and target domains, facilitating domain-invariant feature learning. FDA can be formalized by Eq 1:

$$x^{s \to t} = F^{-1}\left([M_\beta \circ F^A(x^t) + (1 - M_\beta) \circ F^A(x^s), F^P(x^s)]\right) \quad (1)$$

where x^s and x^t are the source and target images respectively. F^A and F^P are amplitude and phase components of Fourier transform F of an RGB image. F^{-1} is the inverse fourier transform. M_β is a mask whose value is zero except for central regions

- Arbitrary Style Transfer Augmentation (Styleaug) [54]: Styleaug is an image augmentation technique that leverages arbitrary style transfer algorithms to generate diverse augmented images by combining the content of one image with the style of another, enhancing the model's ability to generalize across different styles and domains.

Each augmentation can be viewed as representing a distinct domain [55], and incorporating these augmentations into the source training process allows us to enhance the generalization ability of source-only (SO) models. By treating each augmentation as a separate domain, we can simulate a diverse training dataset that covers a wider range of variations and scenarios. This approach helps the transformer model learn to generalize better across different domains, making it more robust and adaptable to unseen data during inference. Eq-2 represents the Augmented image I' obtained through a series of augmentation operations. The notation denotes the composition of augmentation operations, where Aug_n, represents individual augmentation operations applied sequentially. The input image-I undergoes these augmentation operations in the specified order to generate the augmented image I'.

$$I' = Aug_n \circ Aug_{n-1} \circ \ldots \circ Aug_2 \circ Aug_1(I) \quad (2)$$

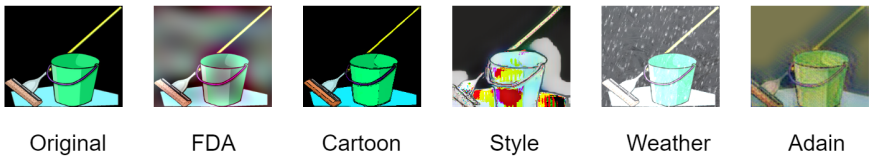

Fig. 2 Augmentations Visualization.

3.2 Key Redundancy

As a next step in our methodology process, we investigate the impact of the key, query, and value components on the performance of transformers. To analyze this, we pass tensors having all elements as 1, shaped to match the input images, through the key, query, and value components of the first layer. The results of our analysis are shown in Table 1 where the element column indicates the element of the 1st attention layer where a tensor having all elements as 1 is passed. We observe that the accuracy drop is minimal when the key component is replaced.

To demonstrate our analysis experiments in the form of an equation, let's consider the input tensor T with dimensions $3 \times 224 \times 224$. The input image is denoted as I. The equation for self-attention can be written as Eq-3:

Table 1 Inference for Key, Query, and Value

Testing	Element	Ar→Cl	Ar→Pr	Ar→Rw	Cl→Ar	Cl→Pr	Cl→Rw	Avg
Baseline		60.6	78.1	83.2	74.3	77.5	80.9	75.8
Ones tensor at input	K	59.3	78.2	82.9	77.4	77	80.5	75.4
	Q	58.4	75.3	81.6	73.5	76.1	79.3	74.0
	V	55.4	73.1	79.2	71.2	75.1	78.1	72.0

$$\text{SelfAttention}(Q_I, K_T, V_I) = \text{softmax}\left(\frac{Q_I \cdot K_T}{\sqrt{d_k}}\right) \cdot V_I \tag{3}$$

Here, Q_I represents the query matrix obtained from the input image I, K_T represents the key matrix obtained from the input tensor T,V_I represents the value matrix obtained from the input image I, and $sqrt(dk)$ represents the square root of the key dimension dk. The self-attention mechanism calculates the attention weights by performing the dot product between the query matrix Q_I and the transposed key matrix ${K_T}^T$, divided by the square root of dk. The resulting attention weights are then passed through a softmax function. Finally, the value matrix V_I is multiplied element-wise with the attention weights to obtain the attended output.

Building upon this observation, we delve deeper into studying key redundancy across different layers of the transformer. To do this, we select a subset of the dataset and determine the range of key values for each layer. Next, we replace the key component with a tensor comprising random values within the previously determined range. By employing this technique, we ensure that replacing the key at any layer does not negatively impact the model's performance.

$$\text{SelfAttention} = \text{softmax}\left(\frac{Q_i R^T}{\sqrt{d_k}}\right) V_i \tag{4}$$

In Eq-4, Q_i represents the i^{th} layer query, R represents the random tensor with the same dimensions as the i^{th} layer key, V_i represents the i^{th} layer value, and the superscript T denotes the transpose operation. The results are shown in Table 2.

Table 2 Inference for Key for different layers of Transformer

SO Model	Testing	Ar→Cl	Ar→Pr	Ar→Rw	Cl→Ar	Cl→Pr	Cl→Rw	Avg
Baseline		60.6	78.1	83.2	74.3	77.5	80.9	75.8
Random Key Tensor(Clean)	Layer 1	60.3	77.9	82.7	73.2	77.1	79.9	75.2
	Layer 2	60.4	77.5	83.5	74	76.7	80.6	75.4
	Layer 5	57	75.7	81.1	67.2	74.5	76.8	72.0
	Layer 6	57.1	76.3	81.4	70.7	75.8	78.1	73.2
	Layer 7	53.6	75.6	81.7	69.4	74.9	78	72.2
	Layer 8	55.6	76.1	81.9	70.3	75.8	78.6	73.0
	Layer 11	56.7	74.8	81	68.8	73.1	77.6	72.0
	Layer 12	58.5	75.9	82.9	70.9	75.1	79.2	73.7

Based on Table 2 the average accuracy drop across different layers is minimal. The baseline average accuracy is 75.8%. The maximum drop in accuracy is observed in layer 5 with a decrease of 3.8%, while the minimal drop is observed in layer 2 with a decrease of 0.4%. This finding opens up opportunities to replace the key component with a domain-specific embedding. By incorporating a domain-specific embedding in place of the key, we potentially enhance the performance of the SO model. This approach enables us to leverage domain-specific information and improve the model's ability to generalize across different domains. By understanding the influence of the key, query, and value components and exploring key redundancy within transformers, we aim to identify strategies that enhance the performance of SO models.

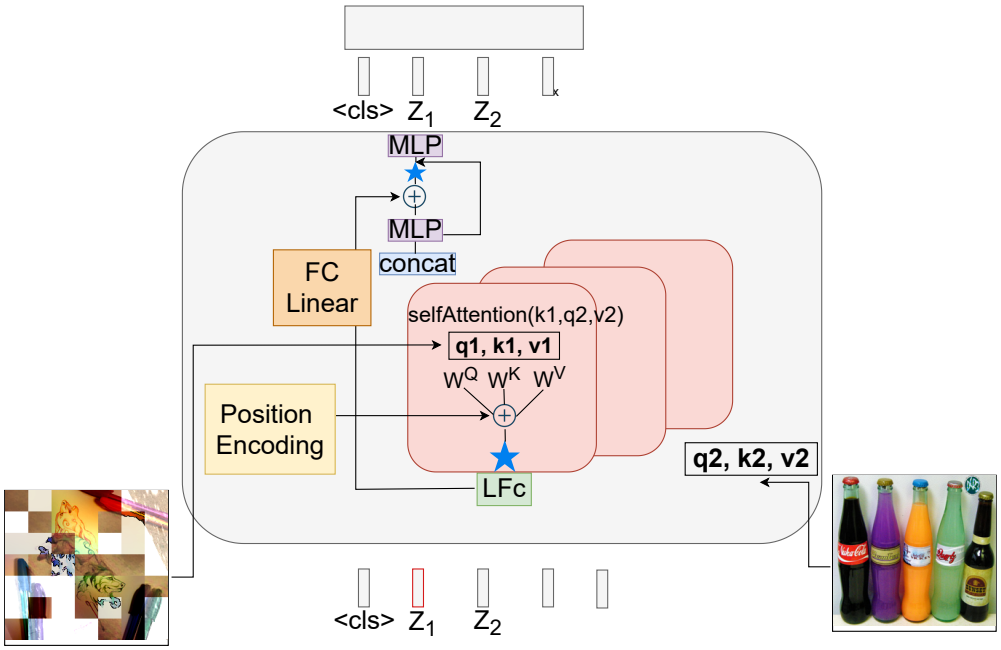

Fig. 3 Illustration of passing DRI in the transformer.

The next step in the methodology framework involves discussing the main contribution of the paper, which is the introduction of a new concept called Domain Representation Image (DRI). As illustrated in Fig .3, the DRI is a domain-specific embedding that is generated for each training image and is included alongside it as an input to the DeiT model. The self-attention module calculates the self-attention between the key from DRI and the value and query from the input image. The paper explores two different possibilities for generating the DRI during the training process:

1. **Single Instance DRI:** In this approach, we use a different image from the same domain and apply the same augmentation as described in Section 3.1. However, we

additionally shuffle the patches within the image. This variation results in a Single Instance DRI, which captures domain-specific information while incorporating patch-level variations within the same domain.

$$\text{RandomAugment} = \text{RandomSelect}([\text{FDA}, \text{AdaIN}, \text{Cartoon}, \text{Weather}, \text{Styleaug}]) \tag{5}$$

$$I_{\text{DRI}} = \text{PatchShuffle}(\text{RandomAugment}(I_d), 16, 16) \tag{6}$$

Eq-5 and Eq-6 encapsulate the crucial steps in the algorithm, integrating the transformation of the DRI image, patch-wise shuffle, and random augmentation selection. In these equations, I_d denotes an image randomly selected from the training set. The function *RandomSelect* enables the random selection of an augmentation function from a given list of augmentations. *RandomAugment* represents the augmentation algorithm that is randomly chosen from the list. The resulting I_{DRI} represents the DRI image with patch-wise shuffle applied, employing a patch size of 16×16. $PatchShuffle$ facilitates the shuffling of patches within the augmented image.

2. **Cross Instance Domain Representation Image (Cross DRI):** For this approach, we combine patches from different images within the same domain, all augmented using the same technique. By merging these patches, we create a Cross DRI that represents a combination of instances within the domain. This allows the model to capture a broader understanding of the domain by incorporating features from multiple images. Algorithm-1 delineates the steps to construct Cross Instance DRI for each input Image while training. It starts by randomly selecting a r number of images from the training set (τ) and applies augmentation (A) to each image. The resulting augmented images are then used to construct the DRI by extracting 16x16 patches randomly from each of them and placing them in the appropriate positions within the DRI. This process continues until the entire DRI is filled with patches from augmented images. The DRI is returned as the final output.

Algorithm 1 Creating a Cross Instance Domain Representation Image

function RandomSelection(τ, r)
    $K \Leftarrow$ empty set
    while $|K| < r$ **do**
        randomly select an image from τ
        add the selected image to K
    end while
    return K
end function

function ApplyAugmentation(A, K)
    $AugmentedImages \Leftarrow$ empty set
    for each image in K **do**
        $AugmentedImage \Leftarrow A$(image)
        add $AugmentedImage$ to $AugmentedImages$
    end for
    return $AugmentedImages$
end function

function InitializeDRI
    $DRI \Leftarrow$ empty image with dimensions $3 \times 224 \times 224$
    return DRI
end function

function GenerateDRI(A, τ, r)
    Input: Augmentation technique A, training set of images τ, number of random images to select r
    Output: Domain Representation Image (DRI)
    $R \Leftarrow$ RandomSelection(τ, r)
    AugmentedImages $\Leftarrow$ ApplyAugmentation(A, R)
    DRI $\Leftarrow$ InitializeDRI()
    $x \Leftarrow 1$
    while $x \leq 224$ **do**
        $y \Leftarrow 1$
        while $y \leq 224$ **do**
            randomIndex $\leftarrow$ RandomSelection($[1, r]$)
            SelectedImage $\leftarrow$ AugmentedImages[randomIndex]
            Patch $\leftarrow$ ExtractPatch(SelectedImage, $x, y, x + 16, y + 16$)
            DRI$[x : x + 15, y : y + 15] \leftarrow$ Patch
            $y \Leftarrow y + 16$
        end while
        $x \Leftarrow x + 16$
    end while
    return DRI
end function

In Algorithm 1, the notations used are as follows:

- τ: The training set of images.
- r: The number of random images to be selected from the training set.
- R: The set of randomly selected images from the training set τ.
- A: The augmentation technique or function applied to each image.
- AugmentedImages: The set of augmented images obtained by applying the augmentation technique A to each image in R.
- DRI: The Domain Representation Image, which is a 3-dimensional image with dimensions $3 \times 224 \times 224$.
- x, y: The coordinates indicate the position of a patch in the DRI image.
- Patch: A patch of dimensions 16×16 extracted from a selected image in the AugmentedImages set.
- ExtractPatch(image, x, y, $x + 16$, $y + 16$): A function that extracts a patch of dimensions 16×16 from the given image at the specified coordinates.

To evaluate the influence of Single Instance DRI and Cross DRI methods on model performance and domain generalization proficiency, we undertake experiments employing both strategies. These methodologies offer divergent insights by infusing domain-specific intelligence into the learning algorithm, thereby facilitating the model's capacity to assimilate and adapt to a spectrum of instances and inherent variations within a unified domain. Throughout the training phase, every image utilized is systematically paired with its respective DRI, be it a Single Instance or a Cross Instance type. This deliberate coupling guarantees that the model concurrently processes the raw image data alongside its domain-specific embeddings. This duality in input not only enriches the learning environment but also empowers the model to navigate and acclimatize to the subtle intricacies and diversities present within the target domain.

Table 3 SO experiments for DRI

SO Model	Ar→Cl	Ar→Pr	Ar→Rw	Cl→Ar	Cl→Pr	Cl→Rw	Avg
Baseline	60.6	78.1	83.2	74.3	77.5	80.9	75.8
DRI Training with augs (2 × 2 shuffle) single-instance	62.8	77.9	83.1	74.2	77.2	79.1	75.72
DRI Training with augs (4 × 4 shuffle) single-instance	61.9	77.9	83.6	74.5	77.5	79.2	75.93
DRI Training with augs (6 × 6 shuffle) single-instance	62.4	77.8	83.4	73.9	77.1	79.8	75.73
DRI Training with augs (8 × 8 shuffle) single-instance	62.8	78.3	83.6	74.5	77.8	79.5	76.08
DRI Training with augs (8 × 8 shuffle), cross-instance(4 img)	62.2	78	83.1	74.5	78	80.5	76.1

We perform experiments with Single Instance DRI, the results of which are shown in Table 3. We find DRI with 8x8 patch shuffling performs the best with an average accuracy of 76.08% which leads us to conclude that 8x8 patch shuffling is the best configuration therefore, we choose this for our Cross DRI SO model which performs even better by giving us an average accuracy of 76.1%. Cross DRI improves the most upon the existing SO baseline and serves as the baseline for the target adaptation experiments that follow in Section 4.

4 Experimental Setup and Results

We demonstrate the efficacy of our work on three standard object recognition DA benchmarks:

1. **Office-Home** [7]: A widely used benchmark in the domain adaptation and computer vision research communities. Fig. 4 represents some of the images used in our experiments from the Office-Home dataset. The dataset comprises approximately 15,500 images divided into 65 classes across four distinct domains: Artistic Images (Ar), Clipart Images (Cl), Product Images (Pr), and Real World (Rw) Images. These domains provide diverse visual content and present unique challenges for domain adaptation algorithms.
2. **Office-31** [8]: Office-31 dataset encompasses 31 object categories distributed across three domains: Amazon (A), DSLR (D), and Webcam (W). These categories represent common office objects such as keyboards, file cabinets, and laptops. The Amazon domain contains approximately 90 images per category, totaling 2817 images. These images were sourced from online merchants' websites, offering a consistent background and scale. The DSLR domain boasts 498 high-resolution images with minimal noise (4288 $\times$ 2848), featuring an average of 5 objects per category, each captured from various viewpoints around three times. In contrast, the Webcam domain comprises 795 low-resolution images (640 $\times$ 480) marked by noticeable noise, color variations, and white balance imperfections.
3. **VisDA-2017** [9]: VisDA-2017 dataset is designed for domain adaptation and consists of over 280,000 images spread across 12 categories in training, validation, and testing domains. The training images are synthetically (S) generated from the same object under various conditions, and the validation images (R) are sourced from the MSCOCO dataset [56].

The experiments are performed on a GeForce RTX 3070 GPU with an AWS-EC2 instance. We utilize Python 3.7.2 and PyTorch as our software environments. These tools, along with the hardware setup, are employed for model training to generate the results presented in this section. To ensure a fair comparison, we follow the experimental settings of CDTrans for source-only training and SHOT for target adaptation and use the DeiT-Base [6], pretrained on ImageNet-1k dataset, as the backbone architecture. The input images are resized to a size of 3 $\times$ 224 $\times$ 224. The DeiT-Base architecture features a configuration of 12 layers, with each layer housing 12 self-attention heads collectively referred to as multi-head self-attention. We maintain an input image size of 224 $\times$ 224 pixels and a patch size of 16 $\times$ 16 pixels throughout

Table 4 Table of parameters

Source-Only Training									
Image size	Patch Size	Number of Tokens	Embedding dimension	Batch Size	Epoch	Learning rate	Weight decay ratio	Momentum	Loss function
3 × 224 × 224	16 × 16	197	768	64	20	3e-3	1e-4	0.9	Cross Entropy with Label Smoothing [57]
Target Adaptation									
Image size	Patch Size	Number of Tokens	Embedding dimension	Batch Size	Epoch	Learning rate	Weight decay ratio	Momentum	Loss function
3 × 224 × 224	16 × 16	197	768	64	15	1e-2	5e-4	0.9	IM Loss [19]

all our experiments. This configuration results in 14 × 14 patches per input image, totaling 196 patches. It's important to note that while DeiT-B includes an additional distillation token, the remainder of the architecture remains consistent with the ViT-B backbone. The training parameters are summarized in Table 4.

Fig. 4 Sample Images from Office-Home Dataset.

To evaluate the results, we use classification accuracy as our metric. Classification accuracy measures the proportion of correctly classified samples over the total number of samples in the dataset. We compare the predicted class labels, $\hat{y}$ obtained by selecting the class with the highest probability for each sample, with the true labels, y, to calculate the accuracy.

$$\hat{y} = argmax\,(P) \tag{7}$$

where, $\hat{y}$ is a vector of predicted class labels of size (N × 1).

To obtain the predicted probabilities, we apply the Softmax function element-wise to the logits, which are the unnormalized output activations obtained from the transformer model, representing the scores for each class. We then apply the Softmax

function to these logits to obtain the predicted probabilities, which are used to compare against the true labels for calculating the classification accuracy:

$$P = softmax\,(Z) \tag{8}$$

where matrix Z has dimensions (N × C), where each element Z_{ij} represents the logit or activation of the i^{th} sample for the j^{th} class and P is the matrix of predicted probabilities, and each element P_{ij} represents the probability of the i^{th} sample belonging to the j^{th} class. The Softmax function is defined as:

$$P_{ij} = \frac{e^{Z_{ij}}}{\sum_{k=1}^{C} e^{Z_{ik}}} \tag{9}$$

Here, $e^{Z_{ij}}$ represents the exponential of the logit Z_{ij}, and $\sum_{k=1}^{C} e^{Z_{ik}}$ represents the sum of exponentials of all logits for the i^{th} sample.

In our evaluation, we compare the results of our proposed method against those of two baseline approaches to gauge the efficacy of our methodology. The comparison involves the following methods:

1. **SHOT**: SHOT, or "Source HypOthesis Transfer," is a framework for unsupervised domain adaptation (UDA). In SHOT, the source model's classifier module remains fixed, while the framework learns a target-specific feature extraction module. This is achieved by utilizing information maximization and self-supervised pseudo-labeling to implicitly align target domain representations with the source hypothesis. SHOT is versatile, applicable to various UDA scenarios. [18]
2. **SHOT++**: An extension of the SHOT framework designed for unsupervised domain adaptation (UDA). It builds upon SHOT's foundation, which utilizes a frozen source classification module and leverages information maximization and self-supervised learning to align target features with the source hypothesis. In addition, SHOT++ introduces a novel labeling transfer strategy, splitting the target data based on prediction confidence and utilizing semi-supervised learning to enhance the accuracy of less-confident predictions in the target domain. [19]
3. **SCLM**: SCLM, or "Semantic Consistency Learning on Manifold," addresses the challenge of leveraging the geometry of target data to solve this complex problem. It focuses on capturing semantic relationships between target data distributed on a manifold. It constructs a Semantic Neighbor Topology (SNT) to capture comprehensive geometric information on the manifold. SCLM utilizes SNT as the basic clustering unit for a new form of deep clustering, with techniques like an entropy regulator and self-supervised learning to ensure the coherent movement of SNT for improved adaptation. [58]
4. **SHOT-B^* (CDTrans)**: This variant, SHOT-B^*, extends the SHOT framework and replaces its backbone architecture with DeiT-base for source-free target adaptation baseline in CDTrans. [10]
5. **CDTrans (NSF)**: CDTrans, or "Cross-Domain Transformer,: tackles the challenge of noisy pseudo-label generation in the target domain by utilizing a two-way center-aware labeling algorithm. It harnesses a non source-free (NSF), weight-sharing

triple-branch transformer framework, leveraging self-attention and cross-attention mechanisms to align source and target domain features while simultaneously learning domain-specific and domain-invariant representations. CDTrans represents one of the first attempts to address UDA tasks with a pure transformer-based approach, demonstrating its potential in overcoming domain adaptation challenges. [10]

Table 5 presents the classification accuracy for Source-Free Domain adaptation on Office-Home. We also present our results on Office-31 [8] and VisDA [9] datasets in Table 6, showcasing the accuracy of the model across various $source \rightarrow target$ scenarios. For example, the $Ar \rightarrow Cl$ column signifies the accuracy of the model in the Clipart domain after being trained on Artistic Images. By analyzing these tables, we aim to highlight the benefits and effectiveness of our proposed method in achieving improved target adaptation results, emphasizing the impact of incorporating DRI in the adaptation process.

The experimental comparison is conducted to evaluate the effectiveness of our proposed method for source-free target adaptation, particularly when incorporating the Domain Representation Image (DRI) in the adaptation process. We compare our target adaptation results with SHOT-B*[10], SHOT++[19], SHOT[18] and SCLM[58]. The experiments are performed on the Cross DRI source-only baseline, where the key element is the integration of DRI during target adaptation. We compare the performance of target adaptation with and without DRI, as well as with the SHOT-B^* baseline.

When performing target adaptation without DRI on the Office-Home dataset, we observe an improvement in accuracy over SHOT-B* and other source-free baselines. Specifically, the accuracy increases from 78.10% to 79.18% as shown in Table-5. However, when incorporating DRI in the key component, we achieve a further improvement in performance. The accuracy rises to 79.58%, demonstrating the effectiveness of including DRI in enhancing the model's adaptability to the target domain. Our model also gives competitive results compared to the non-source-free baseline, CDTrans [10].

This trend of enhanced performance through DRI inclusion extends to other datasets as well. On the Office-31 dataset presented in Table-6, we observe an accuracy increase from 91.4% to 91.8%, which further rises to an impressive 92.3% with DRI in the key component. In the case of the VisDA dataset, our approach similarly excels, with accuracy improving from 85.9% to 86.7% and reaching 87.6% when DRI is incoRporated in the key component.

The findings emphasize the critical role of Domain Representation Images (DRIs), particularly in the key component, in enhancing source-only baseline accuracy during target adaptation. DRIs offer valuable domain-specific insights, improving the model's comprehension of the target domain. They effectively bridge domain gaps, aligning source and target domain understanding, thus achieving better results in the target domain. In summary, DRIs enable deeper target domain understanding, leading to improved generalization, accurate predictions, and better real-world adaptation.

Table 5 Classification Accuracy (%) for SFDA on Office-Home Dataset. * indicates results taken from CDTrans

Method	Ar→Cl	Ar→Pr	Ar→Rw	Cl→Ar	Cl→Pr	Cl→Rw	Pr→Ar	Pr→Cl	Pr→Rw	Rw→Ar	Rw→Cl	Rw→Pr	Avg
SHOT[18]	57.1	78.1	81.5	68.0	78.2	78.1	67.4	54.9	82.2	73.3	58.8	84.3	71.8
SHOT++[19]	57.9	79.7	82.5	68.5	79.6	79.3	68.5	57.0	83.0	73.7	60.7	84.9	73.0
SCLM[58]	58.2	80.3	81.5	69.3	79.0	80.7	69.0	56.8	82.7	74.7	60.6	85.0	73.1
CDTrans (NSF)[10]	68.8	85	86.9	81.5	87.1	87.3	79.6	63.3	88.2	82	66	90.6	80.53
SHOT-B* (CDTrans)[10]	67.1	83.5	85.5	76.6	83.4	83.7	76.3	65.3	85.3	80.4	66.7	83.4	78.1
Cross DRI SO	62.2	78	83.1	74.5	78	80.5	66.5	54.4	79.4	76.3	57	81.5	72.62
Cross DRI + SHOT	68.43	82.02	85.04	77.75	85.36	83.31	77.05	66.8	85.63	81.33	68.57	88.83	**79.18**
Cross DRI + SHOT + DRI Key	69.39	82.09	85.45	78.86	85.81	83.93	77.67	66.44	85.54	81.38	69.69	88.71	**79.58**

Table 6 Classification Accuracy (%) for SFDA on Office-31 and VisDA Dataset. * indicates results taken from CDTrans

Method	Office-31							VisDA
	A→W	D→W	W→D	A→D	D→A	W→A	Avg	S→R
SHOT[18]	90.1	98.4	99.9	94.0	74.7	74.3	88.6	82.9
SHOT++[19]	90.4	98.7	99.9	94.3	76.2	75.8	89.2	87.3
SCLM[58]	95.8	90.0	75.5	98.9	76.0	100.0	89.4	85.3
CDTrans (NSF)[10]	96.7	99.0	100.0	97.0	81.1	81.9	92.6	88.4
SHOT-B* (CDTrans)[10]	94.3	99.0	100.0	95.3	79.4	80.2	91.4	85.9
Cross DRI SO	91.2	95.7	92.9	94.7	75.4	77.3	87.9	81.1
Cross DRI + SHOT	94.8	99.4	99.9	96.0	79.8	80.9	**91.8**	**86.7**
Cross DRI + SHOT + DRI Key	95.4	99.5	100	97.1	81.4	80.6	**92.3**	**87.6**

5 Conclusions

This research marks a significant stride in source-free target adaptation, with the introduction of the Cross Instance Domain Representation Image (Cross DRI) catalyzing a notable ascent in the performance metrics of Vision Transformers across new domains. Our exploration into key redundancy within Vision Transformers not only confirms its presence but also underscores its potential utility in enhancing model adaptability, thereby broadening our comprehension of transformer architectures' nuances in the context of domain generalization.

In light of these contributions, future research endeavors could be channeled towards the refinement of augmentation techniques, emphasizing the generation of more diverse and robust datasets to further strengthen the domain adaptation processes. Moreover, the intrigue surrounding key redundancy in transformers warrants a continued investigative focus, potentially guiding enhancements in model efficiency and adaptation precision.

6 Conflict of Interest and Data Availability

The authors declare that they have no conflict of interest and no known competing financial interests or personal relationships that could have appeared to influence the work reported in this paper.

The data used in this paper is publically available and is already published in [7], [8], [9].

References

[1] Gabriela Csurka. Domain adaptation for visual applications: A comprehensive survey, 2017.

[2] Sicheng Zhao, Xiangyu Yue, Shanghang Zhang, Bo Li, Han Zhao, Bichen Wu, Ravi Krishna, Joseph E Gonzalez, Alberto L Sangiovanni-Vincentelli, Sanjit A Seshia, et al. A review of single-source deep unsupervised visual domain

adaptation. *IEEE Transactions on Neural Networks and Learning Systems*, 33(2):473–493, 2020.

[3] Zhedong Zheng and Yi Yang. Rectifying pseudo label learning via uncertainty estimation for domain adaptive semantic segmentation. *International Journal of Computer Vision*, 129(4):1106–1120, 2021.

[4] Poojan Oza, Vishwanath A Sindagi, Vibashan Vishnukumar Sharmini, and Vishal M Patel. Unsupervised domain adaptation of object detectors: A survey. *IEEE Transactions on Pattern Analysis and Machine Intelligence*, 2023.

[5] Alexey Dosovitskiy, Lucas Beyer, Alexander Kolesnikov, Dirk Weissenborn, Xiaohua Zhai, Thomas Unterthiner, Mostafa Dehghani, Matthias Minderer, Georg Heigold, Sylvain Gelly, et al. An image is worth 16x16 words: Transformers for image recognition at scale. *arXiv preprint arXiv:2010.11929*, 2020.

[6] Hugo Touvron, Matthieu Cord, Matthijs Douze, Francisco Massa, Alexandre Sablayrolles, and Hervé Jégou. Training data-efficient image transformers & distillation through attention. In *International conference on machine learning*, pages 10347–10357. PMLR, 2021.

[7] Hemanth Venkateswara, Jose Eusebio, Shayok Chakraborty, and Sethuraman Panchanathan. Deep hashing network for unsupervised domain adaptation. In *Proceedings of the IEEE conference on computer vision and pattern recognition*, pages 5018–5027, 2017.

[8] Kate Saenko, Brian Kulis, Mario Fritz, and Trevor Darrell. Adapting visual category models to new domains. In *Computer Vision–ECCV 2010: 11th European Conference on Computer Vision, Heraklion, Crete, Greece, September 5-11, 2010, Proceedings, Part IV 11*, pages 213–226. Springer, 2010.

[9] Xingchao Peng, Ben Usman, Neela Kaushik, Judy Hoffman, Dequan Wang, and Kate Saenko. Visda: The visual domain adaptation challenge. arXiv preprint arXiv:1710.06924, 2017.

[10] Tongkun Xu, Weihua Chen, Pichao Wang, Fan Wang, Hao Li, and Rong Jin. Cdtrans: Cross-domain transformer for unsupervised domain adaptation. In *Proceedings of the International Conference on Learning Representations*, 2022.

[11] Konstantinos Bousmalis, Nathan Silberman, David Dohan, Dumitru Erhan, and Dilip Krishnan. Unsupervised pixel-level domain adaptation with generative adversarial networks. In *Proceedings of the IEEE conference on computer vision and pattern recognition*, pages 3722–3731, 2017.

[12] Seiichi Kuroki, Nontawat Charoenphakdee, Han Bao, Junya Honda, Issei Sato, and Masashi Sugiyama. Unsupervised domain adaptation based on source-guided discrepancy. In *Proceedings of the AAAI Conference on Artificial Intelligence*, volume 33, pages 4122–4129, 2019.

[13] Garrett Wilson and Diane J Cook. A survey of unsupervised deep domain adaptation. *ACM Transactions on Intelligent Systems and Technology (TIST)*, 11(5):1–46, 2020.

[14] VS Vibashan, Vikram Gupta, Poojan Oza, Vishwanath A Sindagi, and Vishal M Patel. Mega-cda: Memory guided attention for category-aware unsupervised domain adaptive object detection. In *2021 IEEE/CVF Conference on Computer Vision and Pattern Recognition (CVPR)*, pages 4514–4524. IEEE, 2021.

[15] Kuniaki Saito, Donghyun Kim, Stan Sclaroff, Trevor Darrell, and Kate Saenko. Semi-supervised domain adaptation via minimax entropy. In *Proceedings of the IEEE/CVF international conference on computer vision*, pages 8050–8058, 2019.

[16] Mei Wang and Weihong Deng. Deep visual domain adaptation: A survey. *Neurocomputing*, 312:135–153, 2018.

[17] Pau Panareda Busto and Juergen Gall. Open set domain adaptation. In *Proceedings of the IEEE international conference on computer vision*, pages 754–763, 2017.

[18] Jian Liang, Dapeng Hu, and Jiashi Feng. Do we really need to access the source data? source hypothesis transfer for unsupervised domain adaptation. In *International Conference on Machine Learning*, pages 6028–6039. PMLR, 2020.

[19] Jian Liang, Dapeng Hu, Yunbo Wang, Ran He, and Jiashi Feng. Source data-absent unsupervised domain adaptation through hypothesis transfer and labeling transfer. *IEEE Transactions on Pattern Analysis and Machine Intelligence*, 44(11):8602–8617, 2021.

[20] Yaroslav Ganin, Evgeniya Ustinova, Hana Ajakan, Pascal Germain, Hugo Larochelle, François Laviolette, Mario Marchand, and Victor Lempitsky. Domain-adversarial training of neural networks. *The journal of machine learning research*, 17(1):2096–2030, 2016.

[21] Eric Tzeng, Judy Hoffman, Kate Saenko, and Trevor Darrell. Adversarial discriminative domain adaptation. In *Proceedings of the IEEE conference on computer vision and pattern recognition*, pages 7167–7176, 2017.

[22] Thomas Westfechtel, Hao-Wei Yeh, Qier Meng, Yusuke Mukuta, and Tatsuya Harada. Backprop induced feature weighting for adversarial domain adaptation with iterative label distribution alignment. In *Proceedings of the IEEE/CVF Winter Conference on Applications of Computer Vision*, pages 392–401, 2023.

[23] Mingsheng Long, Yue Cao, Jianmin Wang, and Michael Jordan. Learning transferable features with deep adaptation networks. In *International conference on machine learning*, pages 97–105. PMLR, 2015.

[24] Eric Tzeng, Judy Hoffman, N. Zhang, Kate Saenko, and Trevor Darrell. Deep domain confusion: Maximizing for domain invariance. *ArXiv*, abs/1412.3474, 2014.

[25] Minghao Chen, Hongyang Xue, and Deng Cai. Domain adaptation for semantic segmentation with maximum squares loss. In *Proceedings of the IEEE/CVF International Conference on Computer Vision*, pages 2090–2099, 2019.

[26] Shuhao Cui, Shuhui Wang, Junbao Zhuo, Liang Li, Qingming Huang, and Qi Tian. Towards discriminability and diversity: Batch nuclear-norm maximization under label insufficient situations. In *Proceedings of the IEEE/CVF conference on computer vision and pattern recognition*, pages 3941–3950, 2020.

[27] Ying Jin, Ximei Wang, Mingsheng Long, and Jianmin Wang. Minimum class confusion for versatile domain adaptation. In *Computer Vision–ECCV 2020: 16th European Conference, Glasgow, UK, August 23–28, 2020, Proceedings, Part XXI 16*, pages 464–480. Springer, 2020.

[28] Kuniaki Saito, Kohei Watanabe, Yoshitaka Ushiku, and Tatsuya Harada. Maximum classifier discrepancy for unsupervised domain adaptation. In *Proceedings*

of the IEEE conference on computer vision and pattern recognition, pages 3723–3732, 2018.

[29] Xingchao Peng, Zijun Huang, Yizhe Zhu, and Kate Saenko. Federated adversarial domain adaptation, 2019.

[30] Haozhe Feng, Zhaoyang You, Minghao Chen, Tianye Zhang, Minfeng Zhu, Fei Wu, Chao Wu, and Wei Chen. Kd3a: Unsupervised multi-source decentralized domain adaptation via knowledge distillation. In *ICML*, pages 3274–3283, 2021.

[31] Yan Kang, Yuanqin He, Jiahuan Luo, Tao Fan, Yang Liu, and Qiang Yang. Privacy-preserving federated adversarial domain adaptation over feature groups for interpretability. *IEEE Transactions on Big Data*, 2022.

[32] Lei Song, Chunguang Ma, Guoyin Zhang, and Yun Zhang. Privacy-preserving unsupervised domain adaptation in federated setting. *IEEE Access*, 8:143233–143240, 2020.

[33] Zixuan Qin, Liu Yang, Fei Gao, Qinghua Hu, and Chenyang Shen. Uncertainty-aware aggregation for federated open set domain adaptation. *IEEE Transactions on Neural Networks and Learning Systems*, 2022.

[34] Moslem Yazdanpanah and Parham Moradi. Visual domain bridge: A source-free domain adaptation for cross-domain few-shot learning. In *Proceedings of the IEEE/CVF Conference on Computer Vision and Pattern Recognition*, pages 2868–2877, 2022.

[35] Neerav Karani, Ertunc Erdil, Krishna Chaitanya, and Ender Konukoglu. Test-time adaptable neural networks for robust medical image segmentation. *Medical Image Analysis*, 68:101907, 2021.

[36] Malik Boudiaf, Romain Mueller, Ismail Ben Ayed, and Luca Bertinetto. Parameter-free online test-time adaptation. In *Proceedings of the IEEE/CVF Conference on Computer Vision and Pattern Recognition*, pages 8344–8353, 2022.

[37] Yusuke Iwasawa and Yutaka Matsuo. Test-time classifier adjustment module for model-agnostic domain generalization. *Advances in Neural Information Processing Systems*, 34:2427–2440, 2021.

[38] Xiaofeng Liu, Chaehwa Yoo, Fangxu Xing, C-C Jay Kuo, Georges El Fakhri, Je-Won Kang, and Jonghye Woo. Unsupervised black-box model domain adaptation for brain tumor segmentation. *Frontiers in Neuroscience*, page 341, 2022.

[39] Boris Chidlovskii, Stephane Clinchant, and Gabriela Csurka. Domain adaptation in the absence of source domain data. In *Proceedings of the 22nd ACM SIGKDD International Conference on Knowledge Discovery and Data Mining*, pages 451–460, 2016.

[40] Arun Reddy Nelakurthi, Ross Maciejewski, and Jingrui He. Source free domain adaptation using an off-the-shelf classifier. In *2018 IEEE International conference on big data (Big Data)*, pages 140–145. IEEE, 2018.

[41] Fan Wang, Zhongyi Han, Zhiyan Zhang, and Yilong Yin. Active source free domain adaptation. *ArXiv*, abs/2205.10711, 2022.

[42] Divya Kothandaraman, Sumit Shekhar, Abhilasha Sancheti, Manoj Ghuhan, Tripti Shukla, and Dinesh Manocha. Distilladapt: Source-free active visual domain adaptation. *arXiv preprint arXiv:2205.12840*, 2022.

[43] Baoyao Yang, Andy Jinhua Ma, and Pong C Yuen. Revealing task-relevant

model memorization for source-protected unsupervised domain adaptation. *IEEE Transactions on Information Forensics and Security*, 17:716–731, 2022.

[44] Xiaodong Wang, Junbao Zhuo, Shuhao Cui, and Shuhui Wang. Learning invariant representation with consistency and diversity for semi-supervised source hypothesis transfer. *arXiv preprint arXiv:2107.03008*, 2021.

[45] Ashish Vaswani, Noam Shazeer, Niki Parmar, Jakob Uszkoreit, Llion Jones, Aidan N Gomez, Łukasz Kaiser, and Illia Polosukhin. Attention is all you need. *Advances in neural information processing systems*, 30, 2017.

[46] Jinjing Zhu, Haotian Bai, and Lin Wang. Patch-mix transformer for unsupervised domain adaptation: A game perspective. In *Proceedings of the IEEE/CVF Conference on Computer Vision and Pattern Recognition*, pages 3561–3571, 2023.

[47] Hugo Touvron, Matthieu Cord, Matthijs Douze, Francisco Massa, Alexandre Sablayrolles, and Herve Jegou. Training data-efficient image transformers &; distillation through attention. In *Proceedings of the 38th International Conference on Machine Learning*, pages 10347–10357, 2021.

[48] Jia Deng, Wei Dong, Richard Socher, Li-Jia Li, Kai Li, and Li Fei-Fei. Imagenet: A large-scale hierarchical image database. In *2009 IEEE conference on computer vision and pattern recognition*, pages 248–255. Ieee, 2009.

[49] Olga Russakovsky, Jia Deng, Hao Su, Jonathan Krause, Sanjeev Satheesh, Sean Ma, Zhiheng Huang, Andrej Karpathy, Aditya Khosla, Michael Bernstein, et al. Imagenet large scale visual recognition challenge. *International journal of computer vision*, 115:211–252, 2015.

[50] Yann LeCun, Léon Bottou, Yoshua Bengio, and Patrick Haffner. Gradient-based learning applied to document recognition. *Proceedings of the IEEE*, 86(11):2278–2324, 1998.

[51] Alexander B. Jung et al. imgaug. https://github.com/aleju/imgaug, 2020. Accessed: 2023-11-21.

[52] Xun Huang and Serge Belongie. Arbitrary style transfer in real-time with adaptive instance normalization. In *Proceedings of the IEEE international conference on computer vision*, pages 1501–1510, 2017.

[53] Yanchao Yang and Stefano Soatto. Fda: Fourier domain adaptation for semantic segmentation. In *Proceedings of the IEEE/CVF Conference on Computer Vision and Pattern Recognition*, pages 4085–4095, 2020.

[54] Philip TG Jackson, Amir Atapour Abarghouei, Stephen Bonner, Toby P Breckon, and Boguslaw Obara. Style augmentation: data augmentation via style randomization. In *CVPR workshops*, volume 6, pages 10–11, 2019.

[55] Jogendra Nath Kundu, Akshay Kulkarni, Amit Singh, Varun Jampani, and R Venkatesh Babu. Generalize then adapt: Source-free domain adaptive semantic segmentation. In *Proceedings of the IEEE/CVF International Conference on Computer Vision*, pages 7046–7056, 2021.

[56] Tsung-Yi Lin, Michael Maire, Serge Belongie, James Hays, Pietro Perona, Deva Ramanan, Piotr Dollár, and C Lawrence Zitnick. Microsoft coco: Common objects in context. In *European Conference on Computer Vision*, pages 740–755, 2014.

[57] Christian Szegedy, Vincent Vanhoucke, Sergey Ioffe, Jonathon Shlens, and Zbigniew Wojna. Rethinking the inception architecture for computer vision. In *Proceedings of the IEEE Conference on Computer Vision and Pattern Recognition*, 2016.

[58] Song Tang, Yan Zou, Zihao Song, Jianzhi Lyu, Lijuan Chen, Mao Ye, Shouming Zhong, and Jianwei Zhang. Semantic consistency learning on manifold for source data-free unsupervised domain adaptation. *Neural Networks*, 152:467–478, 2022.